Chemical Geology 534 (2020) 119452

Contents lists available at ScienceDirect

Chemical Geology

journal homepage: www.elsevier.com/locate/chemgeo

Sources and radiocarbon ages of organic carbon in different grain size fractions of Yellow River-transported particles and coastal sediments

Tiantian Ge[a], Yuejun Xue[b], Xueyan Jiang[a], Li Zou[c], Xuchen Wang[a,b,*]

[a] Key Laboratory of Marine Chemistry Theory and Technology, Institute of Advanced Ocean Study, Ocean University of China, Qingdao 266100, China
[b] Center for Isotope Geochemistry and Geochronology, Qingdao National Laboratory for Marine Science and Technology, Qingdao 266237, China
[c] Key Laboratory of Marine Environment and Ecology, College of Environmental Science and Engineering, Ocean University of China, Qingdao 266100, China

ARTICLE INFO

Editor: Jérôme GAILLARDET

Keywords:
Radiocarbon
Stable carbon isotope
Organic matter
Sediment grain size
Yellow River

ABSTRACT

The elemental (TOC, TN and C/N) and carbon isotope ($\Delta^{14}C$ and $\delta^{13}C$) compositions of organic matter were measured in different grain size fractions of particles transported by the Yellow River and surface sediments in the Bohai Sea and the Yellow Sea. In the riverine particle and sediment samples, high OC contents were associated with small grain size fractions consisting mainly of clay minerals. The $\delta^{13}C$ and $\Delta^{14}C$ values of the bulk riverine particulate organic carbon (POC) collected from the Lijin and Xiaolangdi sites were relatively constant but varied significantly (−21.9‰ to −26.0‰ and −325‰ to −620‰, respectively) among the different size fractions. In comparison, large spatial variations in $\delta^{13}C$ (−20.6‰ to −24.5‰) and $\Delta^{14}C$ (−188‰ to −646‰) values, which increased seaward due to the difference in source carbon, were found for bulk TOC $\Delta^{14}C$ preserved in the surface sediments, but no significant differences were observed among the values in the different size fractions in most sediments. The different carbon isotopic values of the riverine POC and sedimentary TOC reflect differences in the sources, degradation and cycling time scales of the OC. The Yellow River exports very old (5220 ± 295 yrs) POC that is much older than the TOC (2457 ± 676 yrs) preserved in the surface sediments in the Bohai and Yellow seas. Calculations using a dual-isotope three end-member model indicate that pre-aged soil OC and ancient fossil OC represent major proportions (57 ± 16% and 30 ± 8%, respectively) of the riverine POC and that terrestrial biomass OC represents a minor proportion (13 ± 11%). The drainage environment of the river plays important roles in controlling the sources and ages of the riverine POC. In contrast, the TOC in the grain size fractions of the surface sediments in the Bohai and Yellow seas is dominated by marine-derived modern OC (47 ± 13%), followed by pre-aged soil OC (29 ± 9%) and ancient fossil OC (25 ± 14%). The ages of the TOC are determined mainly by the source input, rapid sedimentation, sediment minerology and decomposition of OC during early diagenesis in these large river-influenced marginal seas.

1. Introduction

Organic carbon burial in marine sediments represents a major sink of atmospheric CO_2 and plays an important role in carbon cycling, especially in large river-influenced marginal seas (Hedges and Keil, 1995; Burdige, 2005; Blair and Aller, 2012; Bauer et al., 2013). Rivers and their estuaries serve as the principal conduits for the transport of terrigenous sediment to coastal seas, thereby linking the carbon cycles of the terrestrial biosphere and the ocean ecosystem (Milliman and Meade, 1983; McKee et al., 2004; Bianchi and Allison, 2009; Galy and Eglinton, 2011). Globally, approximately 4.5×10^{11} kg of terrestrial organic carbon (OC) is transported by rivers to coastal seas annually, of which 40–50% is in the form of particulates (Ludwig et al., 1996; Hedges et al., 1997). As major sites of river-exported particulate organic carbon (POC) removal, the continental shelves and coastal areas account for approximately 80–90% of OC burial in the ocean (Berner, 1982; Hedges and Keil, 1995; Blair and Aller, 2012), and up to 90% of river-delivered POC could be buried in estuarine and coastal sediments (Aller et al., 1985; Hedges et al., 1997; Burdige, 2005; Bianchi, 2011; Bianchi et al., 2018).

River-transported particles and sediment are often not spatially homogeneous in terms of particle size or chemical characteristics (Keil et al., 1994; Bergamaschi et al., 1997). The quantity and type of POC in the aquatic environment are affected by many factors, such as the source, reactivity, digenetic stage and depositional regime. Great interest exists in the relationships between TOC and different types of

* Corresponding author at: Key Laboratory of Marine Chemistry Theory and Technology, Institute of Advanced Ocean Study, Ocean University of China, Qingdao 266100, China.
E-mail address: xuchenwang@ouc.edu.cn (X. Wang).

https://doi.org/10.1016/j.chemgeo.2019.119452
Received 9 April 2019; Received in revised form 11 December 2019; Accepted 22 December 2019
Available online 30 December 2019

particulate matter, especially in terms of grain size and surface area (Keil et al., 1994; Mayer, 1994a, 1994b; Bergamaschi et al., 1997). In a recent study, Bouchez et al. (2014) measured the radiocarbon age (^{14}C) and stable carbon isotope composition (^{13}C) of POC in different particle size fractions in the Amazon River. They found a general increase in POC content with decreasing particle size, but the POC content was not strongly related to the specific surface areas of the suspended particles. Old rock-derived POC contributed ~10% of the total POC exported by the Amazon River, and the mean age of the POC exported from the Amazon Basin was 1120–2850 years (Bouchez et al., 2014). More recently, Yu et al. (2019b) performed bulk and compound-specific biomarker analyses of suspended particles collected at one site in the low reach (Kenli site) of the Yellow River and found that finer particles (< 32 μm) had higher OC% and lower $\Delta^{14}C$ values of long-chain ($C_{26+28+30}$) fatty acids than the coarser particles, reflecting preferential transport of pre-aged, mineral soil-derived OC in the river.

In marine sediments, Coarse and fine particles are usually not transported in the same manner (Eisma and Li, 1993), which can result in different origins of the fine and coarse particles and sediments. Many studies have demonstrated that high OC burial in sediments is positively correlated with the sedimentation rate and the surface areas of the particles because high sedimentation rates and the large surface areas of fine particles lead to the burial of large amounts of OC in sediments (Keil et al., 1995; Mayer, 1994a, 1994b; Bergamaschi et al., 1997; Curry et al., 2007; Keil and Mayer, 2014). It is widely accepted that fine particles, such as clay minerals with large charged surface areas, have a strong OC adsorption capacity and thus carry and protect high OC abundances in marine sediments (Keil et al., 1994; Hedges et al., 2001; Curry et al., 2007; Keil and Mayer, 2014). In large river-influenced marginal sea sediments, however, interaction of OC and minerals might be more complicated, and the preservation, abundance and reactivity of OC in sediments could be largely influenced by resuspension-deposition loops and sediment redistribution (Bao et al., 2016). Using radiocarbon measurements, Bao et al. (2019) recently reported that contrasting relationships exist between ^{14}C contents of OC and grain size in surface sediments of the Bohai and Yellow seas and are associated with two different hydrodynamic modes. In the deeper regions and erosional areas, bedload transport often decreases the OC ^{14}C contents of the coarser fraction, while resuspension processes result in OC ^{14}C depletion associated with intermediate grain size fractions in the shallow inner-shelf settings. Hydrodynamic processes, overall, play an important role in affecting the ^{14}C heterogeneity of bulk sediments of marginal seas.

The Yellow River is one of the most turbid major rivers in the world. It primarily transports highly erodible fine particles from the Loess Plateau and delivers a large amount of sediment to the Bohai and Yellow Sea (Milliman and Meade, 1983; Milliman and Syvitski, 1992). In order to reduce sediment deposition and increase the discharge carrying capacity in the main channel of the lower Yellow River, the practice of water and sediment regulation (WSR) has been implemented at the Xiaolangdi Reservoir in the river's middle reach since 2002, which has greatly affected the sediment transport in the lower reach of the Yellow River (Zhang et al., 2009; Wang et al., 2016a). In recent years, several studies have focused on WSR events using radiocarbon measurement as a tool to determine the hydrodynamic influence on POC transport in the lower reach of the Yellow River (Tao et al., 2015; Yu et al., 2019a, 2019b). These studies found that, in general, WSR events lead to lower modern OC contribution than periods of natural seasonal variability for river-transported particles.

Although several studies have been conducted using radiocarbon measurement to investigate the sources, transport and cycling of OC in Yellow River-transported particles (Tao et al., 2015; Yu et al., 2019a, 2019b) and adjacent coastal sediment in recent years (Tao et al., 2016; Bao et al., 2016, 2019; Xue et al., 2017), the sampling site of the river particles, however, was very limited and the temporal and spatial variations of OC in the river particles and the hydrodynamic influence on the spatial variability and activities of OC in coastal sediments are still not well understood (Bao et al., 2016). In this paper, we present new radiocarbon and stable carbon isotopic compositions of OC associated with different grain size fractions in suspended particles transported by the Yellow River and in surface sediments of the Yellow River-influenced Bohai Sea and the Yellow Sea. Using a dual isotope three end-member model, we calculated the contribution of the major sources of OC in different size fractions in both riverine POC and sedimentary TOC. We also compared the influence of hydrodynamic sorting on OC transport and preservation during man-made WSR events. These results provide additional insights for better understanding of the importance of transport and supply of terrestrial OC by the Yellow River for regional carbon cycling in marginal seas.

2. Materials and methods

2.1. Study area

The Yellow River is the 2nd largest river in China and the 6th longest (5464 km) river in the world. It originates in the high Qinghai-Tibet Plateau in the far west of China and flows into the Bohai Sea, and it has a drainage area of 7.45×10^9 km^2 (Fig. 1). Delivering ~1×10^9 t/yr sediment to the sea, the Yellow River is well known for its high turbidity and was once ranked the most turbid river in the world (Milliman and Meade, 1983). Most of the Yellow River transported particles are derived from the Chinese Loess Plateau in the middle of the river basin. The Chinese Loess Plateau is one of the largest loess plateaus in the world and occupies approximately half of the whole Yellow River drainage area (Zhang et al., 1990; Liu et al., 2007b; Hirshfield and Sui, 2011). In the last few decades, however, the sediment load of the Yellow River, especially in its lower reach, has been reduced substantially (by ~90%) due to decreased water discharge resulting mainly from the construction of numerous dams and from agricultural irrigation (Walling and Fang, 2003; Wang et al., 2016a). In 2015, the Yellow River delivered 7.26×10^{10} g terrestrial carbon, comprising 57% dissolved organic carbon (DOC) and 43% POC, to the Bohai Sea (Xue et al., 2017).

Both the Bohai Sea and Yellow Sea are shallow semi-enclosed marginal seas in the western North Pacific Ocean (Fig. 1). The Bohai Sea has an area of 77,000 km^2 and is connected to the northern Yellow Sea by the Bohai Strait. The average depth of the Bohai Sea is < 40 m, and it receives a large amount of terrestrial material input mainly from the Yellow River and several small rivers. Relatively high sedimentation rates of 1.62–5.08 mm/yr have been reported for the Bohai Sea (Liu et al., 2007a). The Yellow Sea has an area of ~400,000 km^2 and an average depth of ~60 m. It is bordered by mainland China and the Korean Peninsula (Fig. 1). The Yellow Sea receives a vast amount of sediment input, primarily from the two largest rivers in China, the Yangtze (Changjiang) River and the Yellow River, along with additional inputs from rivers in Korea (Lim et al., 2006). The Yellow River and the Yangtze River together are estimated to discharge approximately 1.6×10^9 tons of sediment annually, accounting for ~10% of the sediment load of all rivers globally (Milliman and Farnsworth, 2011). Fine-grained mud dominates the surface sediments of the shelf areas in the Yellow Sea, although areas of sand and muddy sand are present in the eastern and western parts of the sea (Lim et al., 2007; Yang et al., 2003).

2.2. Sample collection and grain size separation

We collected total suspended particulate matter (SPM) samples from the middle and lower reaches of the Yellow River at two sites, Xiaolangdi and Lijin, which are two hydrographic stations located 600 km and 80 km upstream from the river mouth, respectively (Fig. 1), during the SWR period in June–July 2014. The sediment-water regulation has been a man-controlled annual event since 2002 and is

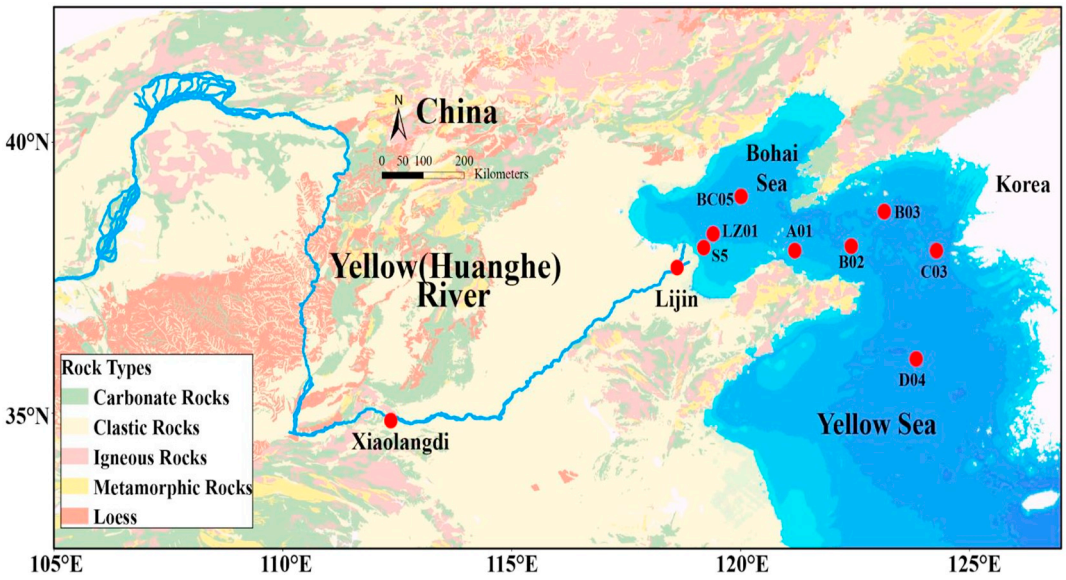

Fig. 1. Map showing the drainage basin of the Yellow River, the two sampling sites in the river's lower reach, the three stations (S5, LZ01, and BC05) in the Bohai Sea and the five stations (A01, B02, B03, C03, and D04) in the Yellow Sea.

Table 1
POC content and isotopic ($\Delta^{14}C$ and $\delta^{13}C$) values measured for SPM and different grain size fractions of SPM collected from Lijin and Xiaolangdi sites in the lower Yellow River in 2014.

Sampling Site	Collection Date	Fraction μm	%	POC %	$\delta^{13}C$ ‰	$\Delta^{14}C$ ‰	^{14}C Age (year BP)
Lijin	2014/6/22	Bulk		0.28	−23.8	−454	4870
		> 63	5	0.14	−24.8	−325	3100
		32–63	26	0.19	−22.9	−590	7160
		16–32	51	0.28	−23.5	−423	4360
		8–16	12	0.37	−23.4	−483	5230
		< 8	6	0.41	−21.9	−417	4280
		Mass balance		0.27	−23.3	−468	
Lijin	2014/7/1	Bulk		0.29	−22.8	−469	5084
		> 63	7	0.15	−22.5	−560	6600
		32–63	24	0.17	−23.2	−423	4360
		16–32	47	0.29	−22.8	−435	4520
		8–16	14	0.36	−22.7	−441	4610
		< 8	8	0.37	−22.8	−473	5080
		Mass balance		0.27	−22.9	−445	
Lijin	2014/7/4	Bulk		0.27	−23.5	−473	5150
		> 63	7	0.13	−23.3	−435	4520
		32–63	22	0.15	−23.1	−493	5390
		16–32	45	0.27	−23.6	−514	5730
		8–16	14	0.33	−22.6	−519	5820
		< 8	12	0.34	−23.4	−493	5400
		Mass balance		0.25	−23.3	−502	
Xiaolangdi	2014/7/5	Bulk		0.30	−23.7	−470	5100
		> 63	3	0.14	−23.0	−536	6100
		32–63	25	0.21	−24.4	−370	3650
		16–32	49	0.44	−23.3	−464	4950
		8–16	16	0.47	−23.6	−469	5020
		< 8	7	0.46	−23.3	−490	5350
		Mass balance		0.38	−23.6	−445	
Xiaolangdi	2014/7/6	Bulk		0.32	−23.3	−508	5700
		> 63	6	0.14	−23.0	−557	6410
		32–63	29	0.15	−23.3	−544	6250
		16–32	50	0.28	−23.4	−501	5520
		8–16	7	0.42	−23.3	−483	5240
		< 8	8	0.47	−22.9	−502	5560
		Mass balance		0.26	−23.3	−516	
Xiaolangdi	2014/7/9	Bulk		0.29	−24.6	−491	5430
		> 63	9	0.15	−26.0	−620	7770
		32–63	23	0.17	−24.1	−441	4610
		16–32	43	0.29	−23.8	−466	4980
		8–16	12	0.43	−23.8	−510	5670
		< 8	13	0.48	−25.5	−419	4290
		Mass balance		0.30	−24.3	−480	

Note: mass balance values were calculated based on the measured percentage of each fraction.

designed to open the dam gate at Xiaolangdi to let the flood water remove the sediment deposited on the lower riverbed and estuary, thus resulting in a high concentration of suspended particles in the river (Wang et al., 2012; Xue et al., 2017). Xiaolangdi station is located below the Xiaolangdi water reservoir, and the samples collected at the beginning of the SWR event represent largely the loess particles transported in the middle reach of the river and deposited recently in the reservoir. Samples collected at the Lijin station, located near the mouth of the Yellow River, represent particles delivered directly to coastal seas by the Yellow River. This study has shown that during the two-week SWR period, SPM flux accounted for 35% of the SPM delivered into the Bohai Sea annually by the Yellow River (Xue et al., 2017). Therefore, samples collected in our study well represent the particles transported in the river and delivered into the coast. We collected six SPM samples during the high flood period on different dates at the two sites (Table 1). Large volumes of water (100 − 200 L) were collected and filtered by vacuum filtration with 140 mm outer diameter (OD) precombusted GF/F filters (0.7 μm, Whatman, 550 °C for 5 h) (Tao et al., 2015). Particles retained on the filters were wrapped in aluminum foil (cleaned and heated to 550 °C) and kept in a refrigerator and transported back to the laboratory for grain size separation. To assess the sources and preservation of the Yellow River-derived POC in the Bohai Sea and the north Yellow Sea, we collected eight surface sediment (0–5 cm) samples, three from the Bohai Sea and five from the Yellow Sea (Fig. 1), using a box grab sampler in August 2013 (Xue et al., 2017). Due to the fast sedimentation rates in the Bohai and Yellow seas, the surface 0–5 cm sediment may not exhibit a large difference in terms of carbon isotope signatures of OC preserved. We kept the sediments frozen at − 20 °C after collection for further processing.

Riverine SPM was separated into five grain size fractions (> 63 μm, 32–63 μm, 16–32 μm, 8–16 μm and < 8 μm) using a hydrodynamic water elutriation method (Supplementary material Fig. S1). This technique has been used in several previous studies for grain size separation of both suspended particles and sediments (Walling and Woodward, 1993; Keil et al., 1998; Wang et al., 2015; Bao et al., 2019; Yu et al., 2019b). We used filtered river water for elutriation circulation driven by a peristaltic pump. When a sampling run was initiated, the water elutriator was filled with clear water. After enough slurry was drawn into the apparatus, clear water was drawn through the system until the sedimentation chambers were completely flushed. Particles with different densities settled in different chambers according to Stokes's Law. The particles from each sedimentation chamber were collected by high-speed centrifugation (10,000 rpm, 20 min). The slurry collected in the outflow containers was left to settle for approximately 72 h, and the particles were then collected by filtration using a 0.7 μm GF/F filter (precombusted at 550 °C for 5 h). All samples were freeze dried for further chemical analysis.

In the laboratory, the surface sediments were thawed at room temperature and wet sieved (with filtered coastal seawater) using a series of stainless-steel sieves. Filtered seawater was poured slowly on top and sediment in the sieves were separated by shaking into four size fractions: 200–500 μm, 100–200 μm, 63–100 μm and < 63 μm (Wheatcroft and Butman, 1997). For sediments collected nearshore such as at S5, BC05 and C03 sites, we found small plant debris large than 500 μm so sediment particles > 500 μm in size (mainly small rocks and plant debris) were discarded. The four separated fractions were freeze dried for further chemical analysis.

2.3. Chemical and isotopic analyses

Total organic carbon (TOC) and total nitrogen (TN) contents were measured for the bulk SPM and sediment samples and their size-separated fractions using a Thermo Flash 2000 Elemental Analyzer. Prior to measurements, the dried and homogenized samples were acidified using 10% HCl at room temperature overnight. After rinsing with Milli-Q water three times, the acidified samples were dried again in an oven at 50 °C and then analyzed for TOC and TN (Komada et al., 2008; Bao et al., 2018). The analytical precision was ± 3% for TOC and ± 4% for TN based on replicate analysis.

We measured both ^{13}C and ^{14}C for the bulk SPM and sediment samples and their size fractions. Samples were first oxidized using a quartz tube oxidation method. Briefly, approximately 50–100 mg (depending on TOC%) of the dried and acidified particulate and sediment samples was placed into a 9 mm OD quartz tube (prebaked at 850 °C for 2 h). After adding C_uO and Ag wire, the quartz tubes were placed under vacuum, flame sealed and combusted at 850 °C for 2 h (Druffel et al., 1992). The resultant CO_2 was collected cryogenically and quantified manometrically on a vacuum line. The purified CO_2 was flame sealed in a 6 mm OD glass tube for isotope analysis.

The $\delta^{13}C$ and $\Delta^{14}C$ measurements were made at the National Ocean Sciences Accelerator Mass Spectrometry (NOSAMS) facility at Woods Hole Oceanographic Institution (WHOI) in the USA and the Center for Isotope Geochemistry and Geochronology (CIGG) at Qingdao National Laboratory for Marine Science and Technology (QNLM) in China. A small split of the CO_2 was analyzed to determine the $\delta^{13}C$ value using an isotope ratio mass spectrometer, and the rest of the CO_2 was graphitized for ^{14}C analysis using an accelerator mass spectrometer (AMS). The $\delta^{13}C$ values are reported in ‰ relative to the Vienna Pee Dee Belemnite (VPDB) and IAEA isotope standards, and the ^{14}C measurements are reported as modern fractions (McNichol et al., 1994). The conventional radiocarbon ages (years before present, BP) were calculated based on Stuiver and Polach (1977). The analytical precision was ± 0.2‰ or better for the $\delta^{13}C$ measurements.

3. Results

3.1. Characteristics of the Yellow River SPM

The POC contents and the carbon isotope compositions ($\delta^{13}C$ and $\Delta^{14}C$) for bulk SPM and each size fraction are summarized in Table 1. The POC contents of the bulk SPM and different size fractions ranged from 0.14% to 0.48% (by dry wt.). There is little difference in the POC contents of the bulk SPM samples collected at Lijin (0.28%) and Xiaolangdi (0.30%). Among the different grain size fractions, the POC contents clearly increase with decreasing grain size in all samples (Fig. 2). The data analysis indicates that overall, a strong positive correlation exists between POC% and grain size for the six SPM samples. Particles in the < 8 μm and 8–16 μm fractions had the highest POC contents.

The $\delta^{13}C$ values of the POC are relatively consistent, ranging from − 22.8‰ to − 24.6‰ for the bulk SPM, with a mean value of − 23.6 ± 0.6‰ (Table 1). The $\delta^{13}C$ values of the different size factions, however, vary from − 21.9‰ to − 26.0‰, with most $\delta^{13}C$ values

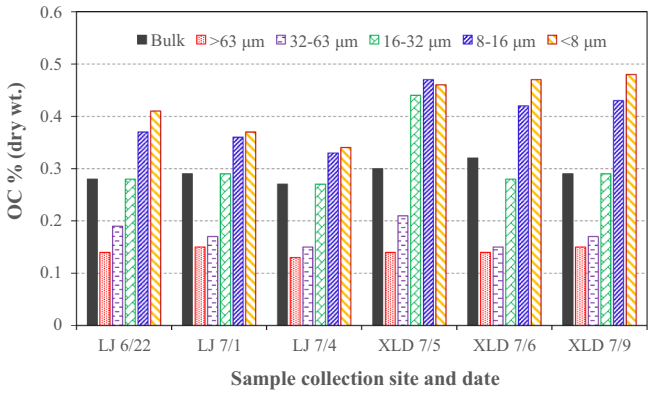

Fig. 2. Organic carbon (OC) contents (% dry wt.) in bulk samples and different grain size fractions of the Yellow River-transported total suspended particulate matter (SPM).

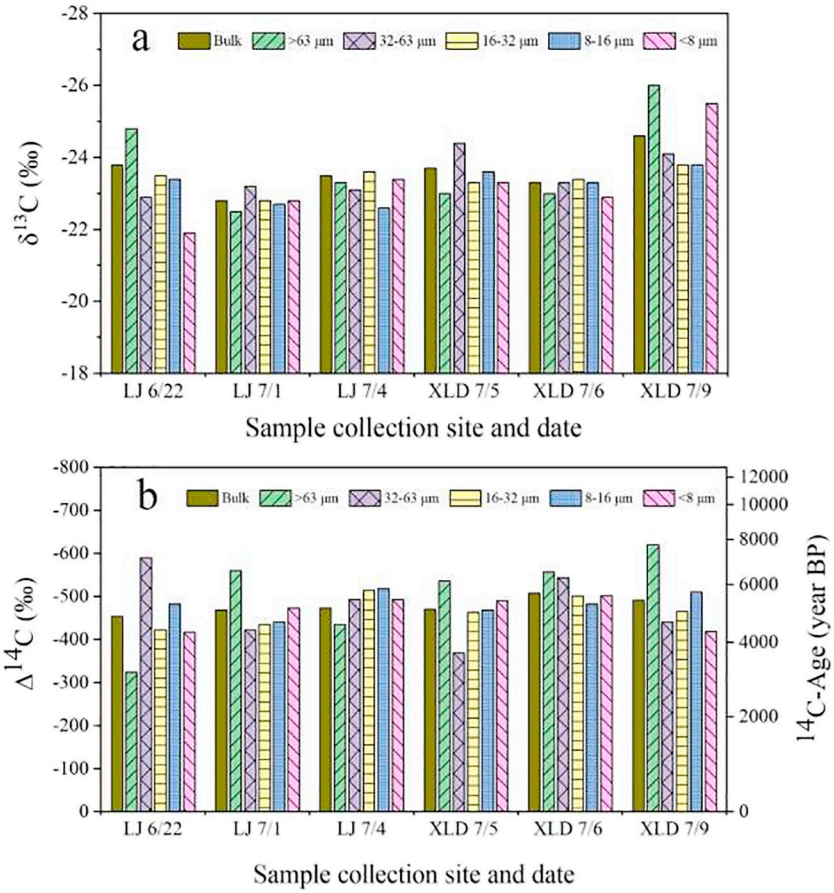

Fig. 3. Plots of (a) $\delta^{13}C$ (‰) values and (b) $\Delta^{14}C$ (‰) values and ^{14}C ages of OC in the bulk samples and different grain size fractions of the Yellow River-transported SPM.

falling in the range between −22.0‰ to −24.0‰ (Fig. 3a). In general, there is no consistent relationship between the $\delta^{13}C$ values and the grain size, unlike the good relationship between POC content and grain size. The $\Delta^{14}C$ values of the bulk SPM POC range from −454‰ to −508‰, corresponding to ^{14}C ages of 4870 to 5700 years before present (yr BP) (Table 1). The $\Delta^{14}C$ values of POC in different size fractions feature a wider range of −325‰ to −691‰, corresponding to ^{14}C ages of 3100 to 7770 yr BP (Table 1, Fig. 3b). The size fraction of > 63 μm in the LJ 7/1 and XLD 7/9 samples contains older POC than the other size fractions (Fig. 3b). In samples LJ 7/1, LJ 7/4 and XLD 7/5, the POC ages, except for the > 63 μm, appear to increase with decreasing size fractions from 32 to 63 μm to < 8 μm. In general, no clear systematic trend between POC age and size fraction exists in the other samples.

The calculated POC content and the isotopic values based on the mass-balance of each size fraction are provided in Table 1. The values were consistent with the measured values of bulk POC and were within 81–103%, 98–100% and 95–106% agreement for OC%, $\delta^{13}C$ and $\Delta^{14}C$, respectively.

3.2. Characteristics of sediment in the Bohai and Yellow seas

The TOC, TN, C/N molar ratio and carbon isotopic composition values measured for the bulk and different size fractions of the surface sediments are summarized in Table 2. The TOC contents (% by dry wt.) range from 0.10 to 0.16%, and the TN contents range from 0.02 to 0.11%. As plotted in Fig. 4a, the TOC contents differ greatly among the sediments. S5, collected in the Yellow River Estuary, has the lowest TOC content (0.15%), and D04, collected in the clay-rich region of the central Yellow Sea, has the highest TOC content (1.11%). B02 and C03, collected in the clay mud area of the northern Yellow Sea, also have relatively high TOC contents (0.89% and 0.53%). The TOC contents in the different grain size fractions in the sediments also vary greatly among the samples (Fig. 4a), but positive correlations between the TOC% and the grain size exist in the sediments of D04, B02, B03 and S5. The TOC% increases with decreasing grain size of the sediments.

The distribution of TN contents in the bulk samples is similar to that of TOC%, with high contents at station D04 (Table 2). As plotted in Fig. 5, a strong linear correlation (R^2 = 0.98, $p < 0.001$) between TOC% and TN% exists for the sediments. The calculated C/N mole ratios of the samples range from 4.2 to 8.4 for all samples (Table 2, Fig. 4b). Sediments S5 and LZ01 from the Yellow River Estuary have lower C/N ratios (4.2–6.5), and BC5 collected in the central Bohai Sea has the highest C/N ratio of 8.4 (Fig. 4b). Sediments collected from the Yellow Sea sites, in general, had similar C/N values (~6–7) for both the bulk samples and different size fractions (Fig. 4b).

The $\delta^{13}C$ values of the TOC range from −20.6‰ to −24.5‰ in the bulk sediments and from −20.2‰ to −23.1‰ in the different size fractions, with the lowest $\delta^{13}C$ value (−24.5‰) of TOC at station S5 at the Yellow River mouth and the highest value (−20.6‰) at station C03 in the Yellow Sea (Fig. 6a). In general, the TOC $\delta^{13}C$ values are relatively consistent in both the bulk samples and the different grain size fractions of the sediments. No clear distribution pattern is observed among the different size fractions (Fig. 6a). The $\Delta^{14}C$ values of the TOC vary greatly among the sediments, ranging from −188‰ to −646‰ in the bulk surface sediments and from −172‰ to −706‰ in the different grain size fractions (Table 2 and Fig. 6b). Station S5 in the Yellow River Estuary has the lowest TOC $\Delta^{14}C$ values (−617‰ to −706‰) and oldest ^{14}C ages of 7640 to 9760 years (BP), while station D04 in the central Yellow Sea has the highest TOC $\Delta^{14}C$ values (−172‰ to −208‰) and youngest ^{14}C ages of 1460 to 1810 years (Table 2 and

Table 2
TOC (%), TN (%), calculated C/N mole ratio and isotopic values ($\Delta^{14}C$ and $\delta^{13}C$) measured for organic matter in different size fractions of the surface sediments collected from the Bohai Sea and the Yellow Sea.

Station #	Location	Sediment type	Fraction (μm)	%	TOC TN (%)	C/N	$\delta^{13}C$ ‰	$\Delta^{14}C$ ‰	^{14}C- Age year (BP)	
S5	37.737°N, 118.758°E	Clay	Bulk		0.15	0.04	4.5	−24.5	−646	8274
			200–500	7	0.08	0.02	4.3	−23.1	−706	9760
			100–200	14	0.10	0.03	4.2	−23.4	−659	8571
			63–100	16	0.12	0.03	4.6	−23.0	−670	8850
			< 63	65	0.19	0.04	5.6	−22.3	−617	7640
			M-balance		0.16	0.04		−23.1	−650	
LZ01	38.055°N, 119.194°E	Clay	Bulk		0.25	0.06	4.8	−22.4	−356	3470
			200–500	6	0.23	0.06	4.4	−22.5	−349	3390
			100–200	18	0.15	0.04	4.8	−22.5	−389	3890
			63–100	18	0.48	0.09	6.5	−22.6	−353	3430
			< 63	58	0.44	0.08	6.4	−22.2	−380	3780
			M-balance		0.35	0.07		−22.3	−375	
BC5	39.000°N, 120.010°E	Clay	Bulk		0.25	0.03	8.4	−22.0	−281	2580
			200–500	3	0.73	0.11	7.5	−21.9	−275	2520
			100–200	10	0.27	0.05	6.1	−22.1	−267	2440
			63–100	23	0.16	0.04	5.1	−22.0	−260	2360
			< 63	64	0.51	0.08	7.0	−21.9	−248	2220
			M-balance		0.41	0.07		−21.9	−253	
A01	38.000°N, 121.183°E	Sand-silt	Bulk		0.30	0.06	6.2	−21.9	−260	2350
			200–500	10	0.36	0.06	6.5	−22.1	−261	2370
			100–200	36	0.29	0.05	6.4	−22.0	−279	2560
			63–100	20	0.28	0.05	6.4	−22.0	−281	2590
			< 63	34	0.33	0.06	6.6	−21.9	−248	2230
			M-balance		0.31	0.05		−22.0	−267	
B02	38.083°N, 122.416°E	Clay-silt	Bulk		0.89	0.15	6.8	−22.2	−234	2080
			200–500	8	0.52	0.10	6.0	−21.4	−245	2200
			100–200	42	0.63	0.11	6.5	−21.3	−231	2050
			63–100	23	0.75	0.13	7.0	−21.5	−227	2000
			< 63	27	0.9	0.15	7.2	−21.4	−230	2040
			M-balance		0.72	0.12		−21.4	−231	
B03	38.722°N, 123.138°E	Sand	Bulk		0.35	0.06	7.2	−21.5	−268	2450
			200–500	16	0.25	0.05	6.4	−21.7	−264	2400
			100–200	44	0.28	0.05	6.7	−21.8	−291	2710
			63–100	25	0.31	0.05	6.9	−21.6	−259	2350
			< 63	15	0.38	0.06	7.0	−21.9	−266	2430
			M-balance		0.30	0.05		−21.7	−275	
C03	38.000°N, 124.277°E	Sand	Bulk		0.53	0.09	6.7	−20.6	−369	3640
			200–500	16	0.60	0.10	6.7	−20.2	−370	3640
			100–200	34	0.42	0.08	6.2	−20.4	−367	3610
			63–100	32	0.64	0.11	7.1	−21.0	−317	3000
			< 63	18	0.62	0.11	6.6	−21.5	−329	3150
			M-balance		0.55	0.10		−20.8	−345	
D04	36.000°N, 123.833°E	Clay	Bulk		1.11	0.17	7.5	−21.7	−188	1610
			200–500	3	1.01	0.16	7.5	−22.0	−208	1810
			100–200	8	1.13	0.18	7.4	−21.7	−199	1720
			63–100	27	1.20	0.18	7.6	−22.2	−186	1590
			< 63	62	1.16	0.18	7.6	−22.3	−172	1460
			M-balance		1.16	0.18		−22.2	−179	

Note: M-balance (mass-balance) values were calculated based on the % of each size fraction.

Fig. 6b). For the sediments from the other sites, the TOC $\Delta^{14}C$ values and ages show less variation and comparable distributions among the size fractions (Fig. 6b). The calculated mass balance values based on the percent of each fraction, in general, agreed well and were within 94–102% and 93–105% of the $\delta^{13}C$ and $\Delta^{14}C$ values of the measured bulk TOC (Table 2).

4. Discussion

4.1. Source of OC in riverine SPM

Although the Yellow River is one of the most turbid rivers in the world, the bulk POC contents (0.27 to 0.32%) of its SPM collected during the WSR period at Xiaolangdi and Lijin stations were low. A study on the seasonal variation of bulk POC at Lijin station in the Yellow River showed that the POC contents varied from 0.2% to 1.07%, and the values in most months were relatively constant (< 0.4%) (Xue et al., 2017). Yu et al. (2019b) found low POC content (0.25–0.32%) at Huayuankou station, which is 120 km downstream from the Xiaolangdi Reservoir. These studies are consistent with our results, indicating that the POC contents transported by the Yellow River are lower than those of most large rivers of the world, such as the Amazon (0.76–1.49%, Bouchez et al., 2014), Yangtze (0.96–1.65%, Wang et al., 2012) and Mississippi (1.02–1.98%, Bianchi et al., 2007). The small difference in the POC contents of the bulk SPM samples collected at Lijin (0.28%) and Xiaolangdi (0.30%) stations indicates that the WSR event has little effect on the bulk POC content. As the primary Loess deposits, due to extensive alteration by chemical and physical weathering over geologic time, the dust from the Loess mountains and desert areas has a low OC% (Zhang et al., 1995; Liu et al., 2007b). Large quantities of fine particles from the Loess Plateau, which occupies approximately half of the entire Yellow River drainage basin in the middle reach of the river, are carried to the lower reaches of the Yellow River (Ran et al., 2013; Zhang et al., 1990). The proportion of the fraction > 32 μm is close to 50% (Zhang et al., 2009; Yu et al., 2019b; Liu et al., 2007b; Wang et al., 2016a), which might contribute to a low bulk POC concentration. The highly turbid water in the Yellow River also limits primary production, which can contribute newly fixed biomass C to the SPM (Zhang et al.,

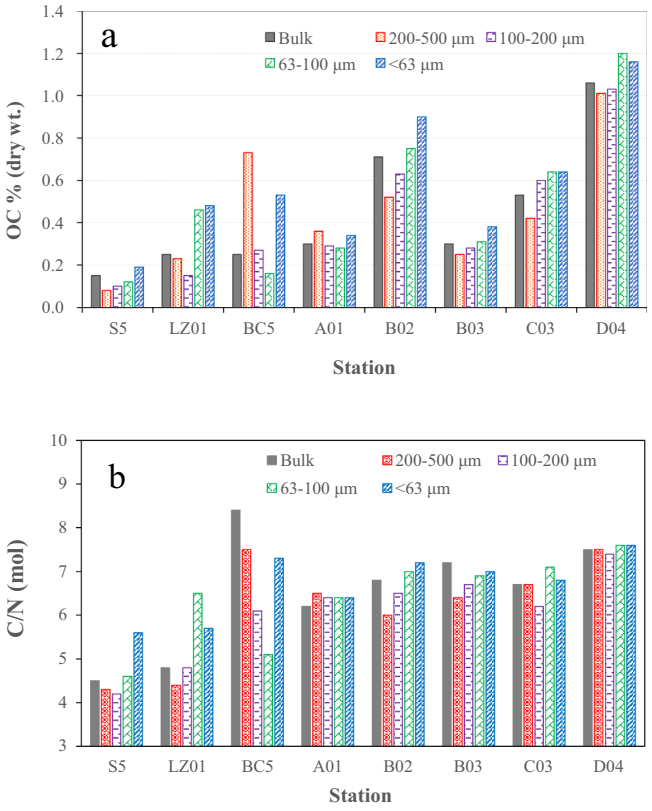

Fig. 4. Plots of (a) OC% in the bulk samples and different grain size fractions of the surface sediments and (b) calculated C/N mole ratios of the bulk samples and different size fractions of the sediments collected from the Bohai and Yellow seas.

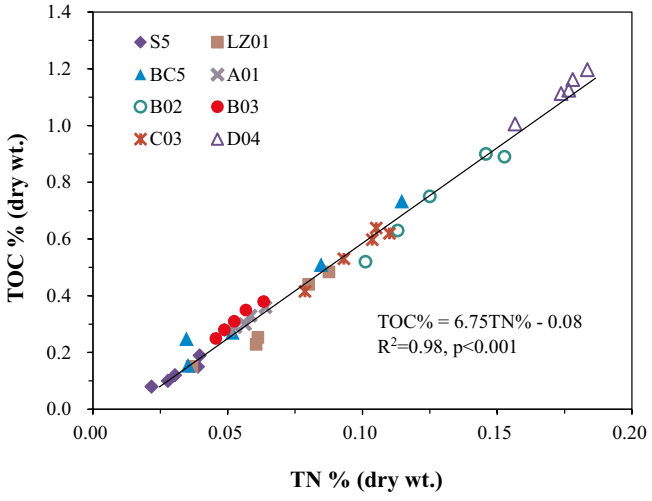

Fig. 5. Plot of TOC% vs. TN% in the bulk samples and different grain size fractions of the surface sediments collected from the Bohai and Yellow seas. The line indicates a linear regression fit to the data.

2013). The relatively homogeneous character of the SPM exported by the Yellow River in terms of its high concentration and low POC content is significantly different from that in other large rivers, such as Amazon, Mississippi and Yangtze, and is mainly influenced by the drainage environment.

The POC contents in the five size fractions of the riverine SPM showed good correlations with particle sizes: small particles (< 8 μm) exhibit higher POC% values than larger particles (Fig. 2). This trend is consistent with the results of previous studies conducted on Yellow River SPM (Tao et al., 2015; Zhang et al., 2009). The association of high OC contents with fine particles is mainly because fine particles, such as clay minerals, have high surface areas and high OC adsorption capacities (Wang and Lee, 1993; Keil et al., 1994; Keil and Mayer, 2014). The fine particles derived from the Loess Plateau include a significant fraction of clay minerals and are delivered into the Yellow River mainly through many small local rivers and streams (Liu et al., 2003, 2007b). The POC content of the fine SPM fraction (< 16 μm) from Xiaolangdi was higher than that from Lijin (Fig. 2), which may be due to the fact that small particles with a large specific surface area easily erode during transportation.

The relatively constant values of POC $\delta^{13}C$ values in the riverine SPM and the size fractions (with averages of 23.6‰ and 23.4‰, respectively) also suggest the similarity and homogeneity of the OC associated with the particles. Yu et al. (2019a) investigated the values of $\delta^{13}C$ with different particle sizes in Kenli station, which is close to Lijin station, and found relatively uniform $\delta^{13}C$ values (-23.7 ± 0.3 to -24.2 ± 0.7‰) with no systematic variations of the $\delta^{13}C$ values among the size fractions, which had a similar range to that of our two stations. The POC $\delta^{13}C$ values we measured are consistent with the values (with an average of -23.3‰, $n = 18$) reported for the loess particles (Liu et al., 2003), further confirming the dominance of loess particles in the Yellow River. The OC associated with the loess particles is very old, with an average ^{14}C age of 5222 ± 295 years. This finding is in good agreement with the results of recent studies that concluded that the Yellow River transports old POC throughout the year (Tao et al., 2015; Xue et al., 2017). In a recent study, Xue et al. (2017) reported the oldest ^{14}C ages of POC (7550 ± 35) in the middle reach of the Yellow River at the Loess Plateau. The OC associated with different size fractions was old, with a ^{14}C age of 3100–7770 years, and exhibited some variation; the > 63 μm fractions of most samples were older than the fine fractions (< 32 μm). and the ages were relatively constant for most size fractions (< 32 μm), as shown in Fig. 3b. The much older OC measured in the > 63 μm and 32–63 μm size fractions likely includes more weathered ancient rock OC that had not broken down to fine particles. This could be the reason why no constant trend between OC age and particle size was found. We also examined the correlations between the $\delta^{13}C$ value and age of POC associated with both bulk SPM and the size fractions and found no clear trend either (data not shown).

4.2. Source of OC in surface sediment

Unlike the POC in the riverine SPM, the TOC preserved in the surface sediments in the Bohai Sea and the Yellow Sea clearly showed some spatial differences. Previous studies showed that TOC generally increased with distance offshore, and the highest values were at the center of muddy areas (Bao et al., 2016, 2019; Tao et al., 2016; Xue et al., 2017). In this study, sediments (D04, C03, B02 and B03) collected in the muddy area of the Yellow Sea had higher TOC contents than sediments (S5 and LZ01) collected in the Yellow River Estuary (Xue et al., 2017). These spatial variations were mainly controlled by the source input of the OC and the hydrodynamic processes (Bao et al., 2016, 2019; Tao et al., 2016; Xue et al., 2017). The Yellow River discharges a large amount of sediment every year, which has a profound effect on the sedimentation of the Bohai and the Yellow seas (Ren and Shi, 1986), resulting in high terrestrial OC deposition and preservation (Bianchi, 2011; Tao et al., 2016). The terrestrial particles with low POC content exported by the Yellow River might have a great dilution effect on the TOC content of sediments in the coastal regions. Sediment deposition in the central Yellow Sea is likely less affected by river discharge, and the higher TOC contents preserved in the sediments are mainly from in situ marine-derived sources, which is consistent with the conclusions of recent studies (Tao et al., 2015; Xue et al., 2017) and is strongly supported by the carbon isotopic values of the TOC (-21.7‰) as discussed below. The C/N ratios for most sediments and their grain

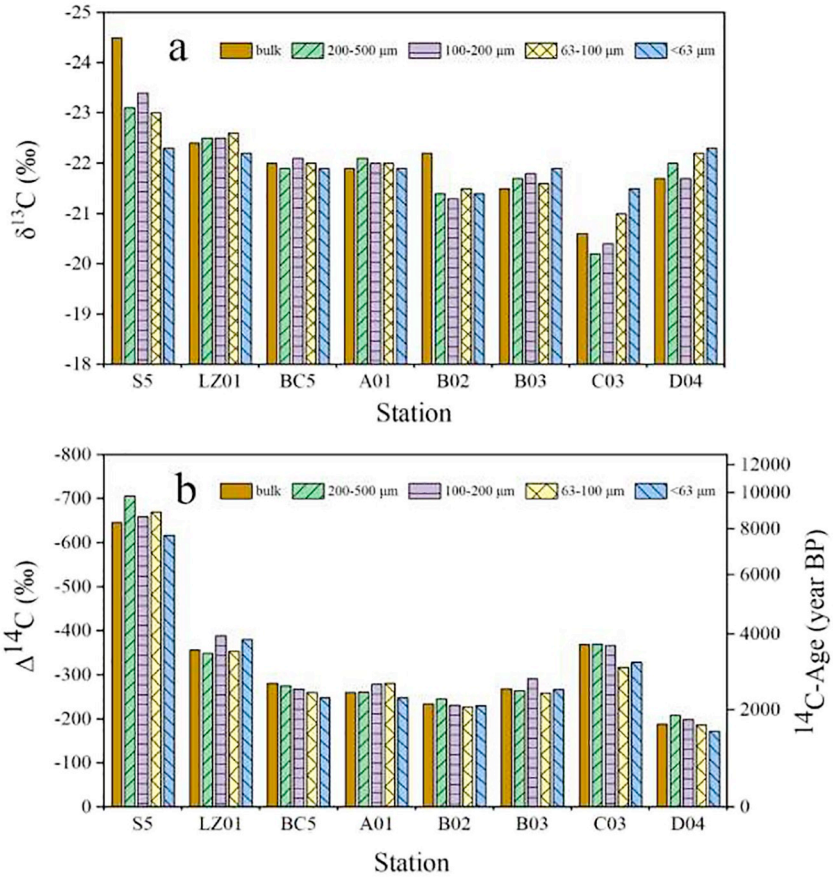

Fig. 6. Plots of (a) $\delta^{13}C$ (‰) values and (b) $\Delta^{14}C$ (‰) values and ^{14}C ages of TOC in the bulk samples and different grain size fractions of the surface sediments collected from the Bohai and Yellow seas.

size fractions are quite consistent, falling between 6.0 and 7.5. These C/N values are similar to the Redfield ratio for marine-derived OC. The strong linear correlation ($R^2 = 0.98$, $p < 0.001$) between TOC and TN for different sediment size fractions (Fig. 5) indicates the copreservation of N (both organic and inorganic N) and OC in the sediments during early diagenesis (Burdige, 2007; Aller et al., 2008). For most sediments studied, the good correlations between TOC% and grain size fraction indicate the importance of fine clay minerals in the adsorption and preservation of OC in the sediments, as has been demonstrated in many other marine sediments (Keil et al., 1994; Mayer, 1994a; Bergamaschi et al., 1997; Curry et al., 2007; Liu and Lee, 2007; Tao et al., 2016).

The carbon isotope values measured for the bulk sediments and their size fractions provide good evidence supporting our conclusions made above. The much younger ages of OC in the sediments of the Yellow Sea (with an average of 2440 years), especially at site D04 (1610 years), compared with the OC age of the mainly river-influenced S5 site (8274 years) indicate that the sediments in the Yellow Sea received significant marine-derived newly fixed OC (Fig. 6b). Their $\delta^{13}C$ values (~ −21‰) are also high and are more similar to marine-derived OC than to riverine OC (−24.5‰). As plotted in Fig. 7, a general correlation exists ($R^2 = 0.35$, $p < 0.05$) showing that the age of the TOC decreases with the TOC% in the different size fractions of the sediments. The correlation is much better ($R^2 = 0.86$, $p < 0.001$) for site S5 (Fig. 7), further indicating that a significant fraction of the OC preserved in the Yellow Sea sediments is from marine OC sources. Megens et al. (2002) reported that the OC in the fine fraction (< 20 μm) had relatively higher $\delta^{13}C$ and $\Delta^{14}C$ values than that in the coarse fractions of surface sediment collected from the Ems-Dollard Estuary in the Netherlands, suggesting that the sources of OC in the fine and coarse fractions were different.

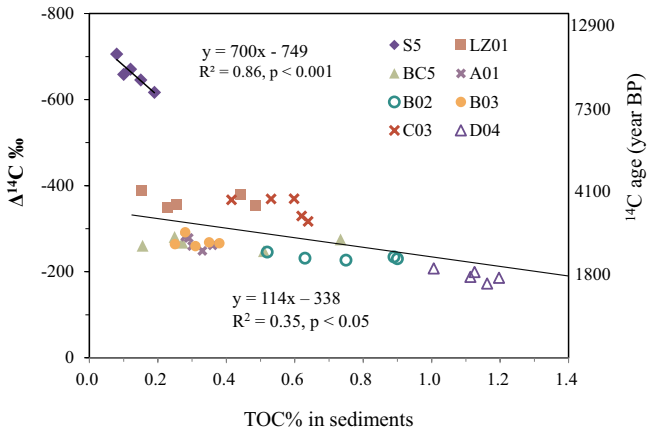

Fig. 7. Plot of $\Delta^{14}C$ (‰) values vs. TOC% in the bulk samples and different grain size fractions of the sediments collected from the Bohai and Yellow seas.

4.3. Contribution of different organic components

To quantitatively calculate the preservation of OC from different sources in the riverine SPM and sediments, we used a dual-isotope three end-member model that has been used for the same application in the Yellow Sea in recent studies (Tao et al., 2015, 2016; Wang et al., 2016b; Xue et al., 2017). The model is based on the following equations:

$$\Delta^{14}C_{OC} = [f_B \times \Delta^{14}C_B] + [f_S \times \Delta^{14}C_S] + [f_F \times \Delta^{14}C_F] \quad (1)$$

$$\delta^{13}C_{OC} = [f_B \times \delta^{13}C_B] + [f_S \times \delta^{13}C_S] + [f_F \times \delta^{13}C_F] \quad (2)$$

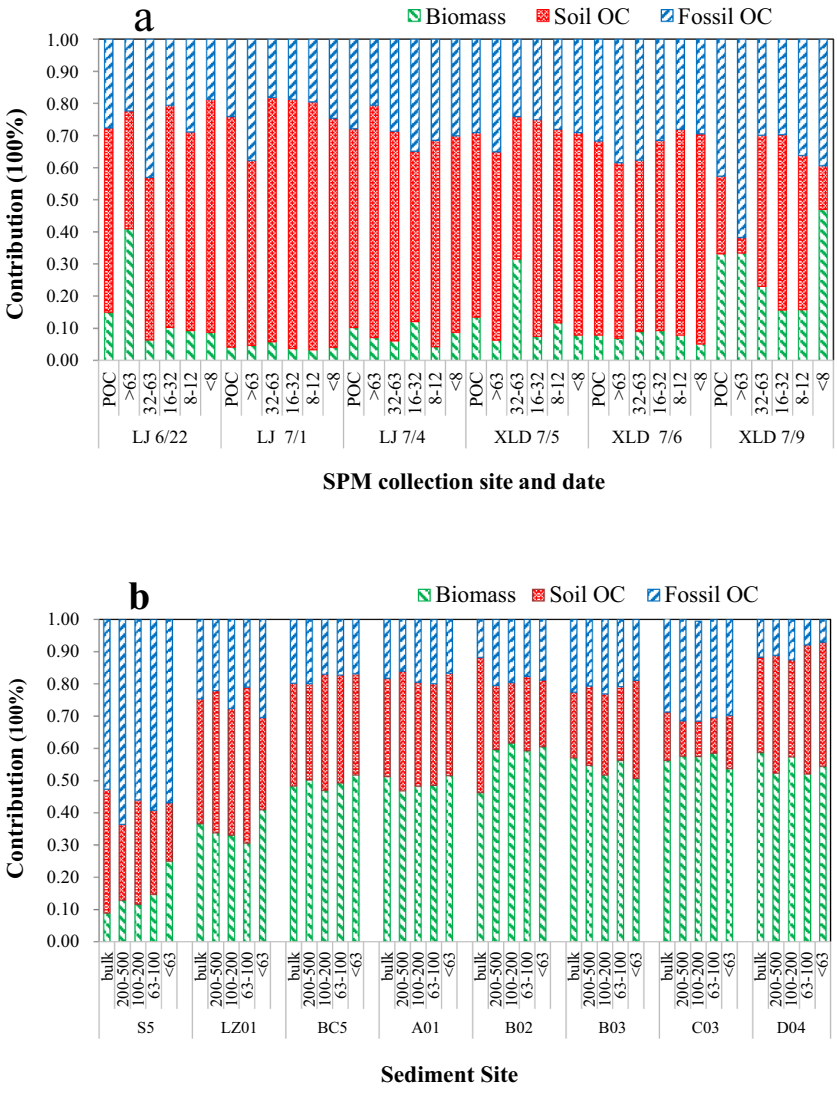

Fig. 8. Plots of the calculated contributions of OC from each end-member to (a) the POC and different size fractions of the Yellow River-transported SPM and (b) bulk TOC and different grain size fractions of the surface sediments of the Bohai and Yellow seas.

$$f_B + f_S + f_F = 1 \quad (3)$$

where $\Delta^{14}C_{OC}$ and $\delta^{13}C_{OC}$ are the measured isotope values of OC in river SPM or sediments. The three end-members are represented by modern biomass (f_B), pre-aged soil OC (f_S), and ancient fossil OC (f_F). To assign the $\Delta^{14}C$ values, we used +40‰ for the modern biomass OC based on the current mean $\Delta^{14}C$ value of atmospheric CO_2 (Zeng et al., 2011; Ishikawa et al., 2015); −320‰ for the pre-aged soil OC based on the values of measured soil OC in the Yellow River basin (Tao et al., 2016; Xue et al., 2017), and −1000‰ for the ancient fossil OC (^{14}C dead OC). However, assigning appropriate $\delta^{13}C$ values for each end-member is more complicated because carbon isotopic fractionation of ^{13}C occurs during organic matter biosynthesis and remineralization (Vogel et al., 1993). In their study, Tao et al. (2015) found that $\delta^{13}C$ values of individual biomarkers (*n*-alkanes) separated from the Yellow River POC could be offset 5–7‰ compared with the $\delta^{13}C$ values of bulk riverine POC. It is therefore necessary to select a range of $\delta^{13}C$ values to cover the most likely variable end-members of measured $\delta^{13}C$ to avoid negative results in the model calculation (Tao et al., 2015, 2016). Here, we used values of −22.4‰ to −24.4‰ for pre-aged soil OC based on the soil OC values measured in the Yellow River basin (Liu et al., 2003; Xue et al., 2017) and −21.1‰ to −25.5‰ for fossil OC (Liu et al., 2007b). To estimate the contribution of biomass OC to river SPM, we used values of −24.0‰ to −30.0‰ for terrestrial C_3 plants, which are the dominant vegetation in the Yellow River basin (Liu et al., 2003). For the sediments, we used values of −18.1‰ to −23.2‰ to cover mostly marine-derived OC in the Yellow Sea (Xue et al., 2017). The model calculation was performed based on a modified Bayesian Markov chain Monte Carlo (MCMC) framework run using MATLAB software (Andersson et al., 2015).

As plotted in Fig. 8, the modern biomass, pre-aged soil OC and ancient fossil OC contributed 3–47%, 14–78% and 18–69% to the bulk POC and its different size fractions of the Yellow River SPM. Except for a few samples, the pre-aged soil OC clearly contributed the majority of the POC in the riverine SPM, followed by the ancient fossil OC and biomass OC (Fig. 8a). For the surface sediment sampling sites except the S5 site, the dominant source of TOC was biomass OC (31–62%), followed by pre-aged soil OC (11–48%) and fossil OC (7–38%) (Fig. 8b). The contribution from each component source did not show significant variations among the size fractions in the sediments. The calculated OC contribution differences between the river SPM and surface sediments again suggest different inputs of OC and preservation processes, supporting our conclusions made above. The calculated large contribution of biomass OC to the surface sediments is likely due to the rapid sedimentation rate of marine-derived organic matter in the shallow coastal water (< 60 m) and fine clay/silt

sediments, which adsorb fresh OC and protect it from microbiol degradation (Keil et al., 1994; Keil and Mayer, 2014). The old refractory soil OC and fossil OC associated with SPM exported by the Yellow River are deposited and preserved in the sediments of the Bohai and Yellow seas, thus indicating that a major sink in the carbon budget exists in China's marginal seas (Tao et al., 2015, 2016; Bao et al., 2016, 2019; Xue et al., 2017). As reported by Bao et al. (2019), the hydrodynamic sorting and resuspension-deposition processes could affect the ^{14}C heterogeneity of bulk sediments of the Bohai, Yellow and East China seas but cannot actually change the age of the very old OC that is likely due to the weathering of fossil OC along the Yellow River basin and delivery to the coasts.

5. Conclusions

The Yellow River transports and exports low concentrations (< 0.48%) of very old (~4500 years) POC. High OC% values are associated with fine clay minerals. The $\delta^{13}C$ and $\Delta^{14}C$ values of the POC are relatively consistent (−22.8 to −24.6‰ and − 454 to −508‰, respectively) in the bulk riverine SPM but vary among the different grain size fractions in river particles (−21.9 to −26.0‰ and −325 to −620‰, respectively). Our model calculations indicate that pre-aged soil OC (57 ± 16%) and ancient fossil OC (30 ± 8%) are the dominant components and that terrestrial vegetation contributes little (13 ± 11%) OC to the POC in the riverine SPM. The general low OC% values and carbon isotope values in the riverine SPM suggest that extensively degraded loess particles dominate the SPM in the lower reach of the Yellow River.

Higher TOC values are also associated with small grain size fractions in the surface sediments of the Bohai Sea and the Yellow Sea. Although the values of $\delta^{13}C$ are relatively consistent (−22.0 ± 1.1‰) for the TOC preserved in the surface sediments, large spatial variations in the $\Delta^{14}C$ values and ^{14}C ages (1460 to 8270 yr) are observed in the sediments, indicating the deposition and preservation of OC from different sources. A major fraction of the TOC is contributed by marine-derived OC (47 ± 13%), followed by pre-aged soil OC (29 ± 9%) and ancient fossil OC (25 ± 14%) in the different grain size fractions of the sediments in the Bohai Sea and the Yellow Sea. Our study also suggests that the use of $\delta^{13}C$ values alone has limitations when attempting to identify sources of OC preserved in coastal sediments, especially in areas influenced by large rivers. The use of the radiocarbon ages of the OC can overcome these shortcomings.

Supplementary data to this article can be found online at https://doi.org/10.1016/j.chemgeo.2019.119452.

Declaration of competing interest

The authors declare that they have no known competing financial interests or personal relationships that could have appeared to influence the work reported in this paper.

Acknowledgments

We thank Qian Liu for help during the river SPM sampling and Yuanzhi Qi, Sen Dan and Chunle Luo for laboratory assistance. We also thank the staff at the National Ocean Science Accelerator Mass Spectrometry (NOSAMS) facility and the Center for Isotope Geochemistry and Geochronology (CIGG) for high precision measurements of the $\delta^{13}C$ and $\Delta^{14}C$ values of the samples. Financial support for this work was provided by the National Natural Science Foundation of China (Grants #41776082 and 41476057 to XCW).

References

Aller, R.C., Mackin, J.E., Ullman, W.J., Wang, C.H., Tsai, S.M., Cai, J.J., Sui, Y.N., Hong, J.Z., 1985. Early chemical diagenesis, sediment-water solute exchange, and storage of reactive organic matter near the mouth of the Changjiang, East China Sea. Cont. Shelf Res. 4, 227–251.

Aller, R.C., Blair, N.E., Brunskill, G.J., 2008. Early diagenetic cycling, incineration, and burial of sedimentary organic carbon in the central Gulf of Papua (Papua New Guinea). J. Geophys. Res. Earth Surf. 113, 1–22.

Andersson, A., Deng, J., Du, K., Zheng, M., Yan, C., Sköld, M., Gustafsson, Ö., 2015. Regionally-varying combustion sources of the January 2013 severe haze events over eastern China. Environ. Sci. Technol. 49, 2038–2043.

Bao, R., Mcintyre, C., Zhao, M., Zhu, C., Kao, S.J., Eglinton, T.I., 2016. Widespread dispersal and aging of organic carbon in shallow marginal seas. Geology 44, 791–794.

Bao, R., McNichol, A.P., Hemingway, J.D., Lardie, G.M.C., Eglinton, T.I., 2018. The effect of different acid-treatments on the radiocarbon age spectrum of organic matter in sediments determined by Ramped PyrOx/Accelerator Mass Spectrometry. Radiocarbon 61, 395–413.

Bao, R., Blattmann, T.M., Mclntyre, C., Zhao, M.X., Eglinton, T.I., 2019. Relationships between grain size and organic carbon ^{14}C heterogeneity in continental margin sediments. Earth planet sc. Let. 505, 76–85.

Bauer, J.E., Cai, W.J., Raymond, P.A., Bianchi, T.S., Hopkinson, C.S., Regnier, P.A., 2013. The changing carbon cycle of the coastal ocean. Nature 504, 61–70.

Bergamaschi, B.A., Tsamakis, E., Keil, R.G., Eglinton, T.I., Montluçon, D.B., Hedges, J.I., 1997. The effect of grain size and surface area on organic matter, lignin and carbohydrate concentration, and molecular compositions in peru margin sediments. Geochim. Cosmochim. Acta 61 (6), 1247–1260.

Berner, R.A., 1982. Burial of organic carbon and pyrite sulfur in the modern ocean: its geochemical and environmental significance. Am. J. Sci. 282, 451–473.

Bianchi, T.S., 2011. The role of terrestrially derived organic carbon in the coastal ocean: a changing paradigm and the priming effect. Natl. Acad. Sci. U.S.A. 108, 19473–19481.

Bianchi, T.S., Allison, M.A., 2009. Large-river delta-front estuaries as natural "recorders" of global environmental change. Natl. Acad. Sci. U.S.A. 106, 8085–8092.

Bianchi, T.S., Wysocki, L.A., Stewart, M., Filley, T.R., McKee, B.A., 2007. Temporal variability in terrestrially-derived sources of particulate organic carbon in the lower Mississippi River and its upper tributaries. Geochim. Cosmochim. Acta 71, 4425–4437.

Bianchi, T.S., Cui, X., Blair, N.E., Burdige, D.J., Eglinton, T.I., Galy, V., 2018. Centers of organic carbon burial and oxidation at the land-ocean interface. Org. Geochem. 115, 138–155.

Blair, N.E., Aller, R.C., 2012. The fate of terrestrial organic carbon in the marine environment. Annu. Rev. Mar. Sci. 4, 401–423.

Bouchez, J., Galy, V., Hilton, R.G., Gaillardet, J., Moreira-Turcq, P., Andrea Perez, M., France-Lanord, C., Maurice, L., 2014. Source, transport and fluxes of Amazon River particulate organic carbon: Insights from river sediment depth-profiles. Geochim. Cosmochim. Acta 133, 280–298.

Burdige, D.J., 2005. Burial of terrestrial organic matter in marine sediments: a re-assessment. Glob. Biogeo. Cycles 19, 922–932.

Burdige, D.J., 2007. Preservation of organic matter in marine sediments: controls, mechanisms, and an imbalance in sediment organic carbon budgets? Chem. Rev. 107, 467–485.

Curry, K.J., Bennett, R.H., Mayer, L.M., Curry, A., Abril, M., Biesiot, P.M., Hulbert, M.H., 2007. Direct visualization of clay microfabric signatures driving organic matter preservation in fine-grained sediment. Geochim. Cosmochim. Acta 71, 1709–1720.

Druffel, E.R., Williams, P.M., Bauer, J.E., Ertel, J.R., 1992. Cycling of dissolved and particulate organic matter in the open ocean. J. Geophys. Res. 97, 15,639–15,659.

Eisma, D., Li, A., 1993. Changes in suspended-matter floc size during the tidal cycle in the dollard estuary. Netherlands Journal of Sea Research 31 (2), 107–117.

Galy, V., Eglinton, T., 2011. Protracted storage of biospheric carbon in the Ganges-Brahmaputra basin. Nat. Geosci. 16. https://doi.org/10.1038/NGEO1293.

Hedges, J.I., Keil, R.G., 1995. Sedimentary organic matter preservation: an Assessment and speculative synthesis. Mar. Chem. 49 (2–3), 81–115.

Hedges, J.I., Keil, R.G., Benner, R., 1997. What happens to terrestrial organic matter in the ocean? Org. Geochem. 27, 195–212.

Hedges, J.I., Baldock, J.A., Gélinas, Y., Lee, C., Peterson, M., Wakeham, S.G., 2001. Evidence for non-selective preservation of organic matter in sinking marine particles. Nature 409, 801–804.

Hirshfield, F., Sui, J., 2011. Changes in sediment transport of the Yellow River in the Loess Plateau. In: Ginsberg, S.S. (Ed.), Sediment Transport. InTech, pp. 198–213.

Ishikawa, N., Tayasu, I., Yamane, M., Yokoyama, Y., Sakai, S., Ohkouchi, N., 2015. Sources of dissolved inorganic carbon in two small streams with different bedrock geology: insights from carbon isotopes. Radiocarbon 57 (3), 439–448.

Keil, R.G., Mayer, L.M., 2014. Mineral matrices and organic matter. Reference Module in Earth Systems and Environmental Sciences 12, 337–359.

Keil, R.G., Montluçon, D.B., Prahl, F.G., Hedges, J.I., 1994. Sorptive preservation of labile organic matter in marine sediments. Nature 370 (6490), 549–552.

Keil, R.G., Tsamakis, E., Giddings, J.C., Hedges, J.I., 1995. Biochemical distributions (amino acids, neutral sugars, and lignin phenols) among size-classes of modern marine sediments from the Washington coast. Geochim. Cosmochim. Acta 62, 1347–1364.

Keil, R.G., Tsamakis, E., Giddings, J.C., Hedges, J.I., 1998. Biochemical distributions (amino acids, neutral sugars, and lignin phenols) among size-classes of modern marine sediments from the Washington coast. Geochim. Cosmochim. Acta 62, 1347–1364.

Komada, T., Anderson, M.R., Dorfmeier, C.L., 2008. Carbonate removal from coastal sediments for the determination of organic carbon and its isotopic signatures, $\delta^{13}c$ and $\Delta^{14}c$: comparison of fumigation and direct acidification by hydrochloric acid. Limnol. oceanogr-Meth. 6 (6), 254–262.

Lim, D.I., Jung, H.S., Choi, J.Y., Yang, S., Ahn, K.S., 2006. Geochemical compositions of river and shelf sediments in the yellow sea: grain-size normalization and sediment provenance. Cont. Shelf Res. 26 (1), 15–24.

Lim, D.I., Choi, J.Y., Jung, H.S., Rho, K.C., Ahn, K.S., 2007. Recent sediment

accumulation and origin of shelf mud deposits in the yellow and east china seas. Prog. Oceanogr. 73 (2), 145–159.
Liu, Z.F., Lee, C., 2007. The role of organic matter in the sorption capacity of marine sediments. Mar. Chem. 105, 240–257.
Liu, W., An, Z., Zhou, W., Head, Head, M.J., Cai, D., 2003. Carbon isotope and C/N ratios of suspended matter in rivers: An indicator of seasonal change in C4/C3 vegetation. Appl. Geochem. 18, 1241–1249.
Liu, J.G., Li, A.C., Xu, Z.K., Xu, F.J., 2007a. Manganese abnormity in Holocene sediments of the Bohai Sea. J. China Univ Geosic. 18 (2), 135–141.
Liu, W., Yang, H., Ning, Y., An, Z., 2007b. Contribution of inherent organic carbon to the bulk $\delta^{13}C$ signal in loess deposits from the arid western Chinese loess plateau. Org. Geochem. 38 (9), 1571–1579.
Ludwig, W., Probst, J.L., Kempe, S., 1996. Predicting the oceanic input of organic carbon by continental erosion. Glob. Biogeochem. Cycles 10 (1), 23–41.
Mayer, L.M., 1994a. Relationships between mineral surfaces and organic carbon concentrations in soils and sediments. Chem. Geol. 114 (3–4), 347–363.
Mayer, L.M., 1994b. Surface area control of organic carbon accumulation in Continental shelf sediments. Geochimi. Cosmochim. Acta 58, 1271–1284.
McKee, B.A., Aller, R.C., Allison, M.A., Bianchi, T.S., Kineke, G.C., 2004. Transport and transformation of dissolved and particulate materials on continental margins influenced by major rivers: benthic boundary layer and seabed processes. Cont. Shelf Res. 24, 899–926.
McNichol, A.P., Jones, G.A., Hutton, D.J., Gagnon, A.R., 1994. The rapid Preparation of seawater P_{CO2} for radiocarbon analysis at the national ocean sciences AMS facility. Radiocarbon 36, 237–246.
Megens, L., Plicht, J.V.D., Leeuw, J.W.D., Smedes, F., 2002. Stable carbon and radiocarbon isotope compositions of particle size fractions to determine origins of sedimentary organic matter in an estuary. Org. Geochem. 33 (8), 945–952.
Milliman, J.D., Farnsworth, K.L., 2011. River Discharge to the Coastal Oceans: A Global Synthesis. Cambridge University Press, New York.
Milliman, J.D., Meade, R.H., 1983. World-wide delivery of river sediment to the oceans. J. Geol. 91 (1), 1–21.
Milliman, J.D., Syvitski, J.P.M., 1992. Geomorphic/tectonic control of sediment discharge to the ocean: the importance of small mountainous rivers. J. Geol. 100 (5), 525–544.
Ran, L., Lu, X.X., Sun, H., Han, J., Li, R., Zhang, J., 2013. Spatial and seasonal variability of organic carbon transport in the Yellow River, China. J. Hydrol. 498, 76–88.
Ren, M.E., Shi, Y.L., 1986. Sediment discharge of the Yellow river (China) and its effect on the sedimentation of the Bohai and the Yellow sea. Cont. Shelf Res. 6 (6), 785–810.
Stuiver, M., Polach, H.A., 1977. Discussion: Reporting of ^{14}C data. Radiocarbon 19, 355–363.
Tao, S., Eglinton, T.I., Montluçon, D.B., Mcintyre, C., Zhao, M., 2015. Pre-aged soil organic carbon as a major component of the yellow river suspended load: regional significance and global relevance. Earth Planet. Sci. Lett. 414, 77–86.
Tao, S., Eglinton, T.I., Montluçon, D.B., Mcintyre, C., Zhao, M., 2016. Diverse origins and pre-depositional histories of organic matter in contemporary Chinese marginal sea sediments. Geochim. Cosmochim. Acta 191, 70–88.
Vogel, J.C., Ehleringer, J.R., Hall, A.E., Farquhar, G.D., 1993. Variability of carbon isotope fractionation during photosynthesis. In: Ehleringer, J.R., Hall, A.E., Farquhar, G.D. (Eds.), Stable Isotopes and Plant Carbon-Water Relations. Academic Press, San Diego, pp. 29–46.
Walling, D.E., Fang, D., 2003. Recent trends in the suspended sediment loads of the world's rivers. Glob. Planet. Change 39, 111–126.
Walling, D.E., Woodward, J.C., 1993. Use of a field-based water elutriation system for monitoring the in situ particle size characteristics of fluvial suspended sediment. Water Res. 23 (9), 1413–1421.
Wang, X.C., Lee, C., 1993. Adsorption and desorption of aliphatic amines, amino acids and acetate by clay minerals and marine sediments. Mar. Chem. 44 (1), 1–23.
Wang, X., Ma, H., Li, R., Song, Z., Wu, J., 2012. Seasonal fluxes and source variation of organic carbon transported by two major Chinese Rivers: the Yellow River and Changjiang (Yangtze) River. Glob. Biogeochem. Cycles 26, GB2025.
Wang, J.P., Yao, P., Bianchi, T.A., Li, D., Zhao, B., Cui, X.Q., Pan, H.H., Zhang, T.T., Yu, Z.G., 2015. The effect of particle density on the sources, distribution, and degradation of sedimentary organic carbon in the Changjiang Estuary and adjacent shelf. Chem. Geo. 402, 52–67.
Wang, S., Fu, B., Piao, S., Lu, Y., Ciais, P., Feng, X., Wang, Y., 2016a. Reduced sediment transport in the Yellow River due to anthropogenic changes. Nat. Geosci. 9, 38–42.
Wang, X., Xu, C., Druffel, E.M., Qi, Y., Xue, Y., 2016b. Two black carbon pools transported by the Changjiang and Huanghe Rivers in China. Global Biogeochem. Cycles 30, 1778–1790.
Wheatcroft, R.A., Butman, C.A., 1997. Spatial and temporal variability in aggregated grain-size distributions, with implications for sediment dynamics. Cont. Shelf Res. 17 (4), 367.
Xue, Y.J., Zou, L., Ge, T.T., Wang, X.C., 2017. Mobilization and export of millennial-aged organic carbon by the yellow river. Limnol. Oceanogr. 62, 95–111.
Yang, S.Y., Jung, H.S., Lim, D.I., Li, C.X., 2003. A review on the provenance discrimination of sediments in the yellow sea. Earth-Sci Rev. 63 (1), 93–120.
Yu, M., Eglinton, T.I., Haghipour, N., Montlucon, D.B., Wacker, L., Hou, P., Zhang, H., Zhao, M., 2019a. Impacts of natural and human-induced hydrological variability on particulate organic carbon dynamics in the Yellow River. Environ. Sci. Technol. 53, 1119–1129.
Yu, M., Eglinton, T.I., Haghipour, N., Montlucon, D.B., Wacker, L., Wang, Z., Jin, G., Zhao, M.X., 2019b. Molecular isotopic insights into hydrodynamic controls on fluvial suspended particulate organic matter transport. Geochim. Cosmochim. Acta 262, 78–91.
Zeng, F.W., Masiello, C.A., Hockaday, W.C., 2011. Controls on the origin and cycling of riverine dissolved inorganic carbon in the brazos river, Texas. Biogeochemistry 104 (1), 275–291.
Zhang, L.J., Huang, W.W., Shi, M.C., 1990. Huanghe (Yellow river) and its estuary: sediment origin, transport and deposition. J. Hydrol. 120 (1), 203–223.
Zhang, J., Huang, W.W., Etolle, R.L., Jusserand, C., 1995. Major element chemistry of the Huanghe (Yellow River), China - weathering processes and chemical fluxes. J. Hydrol. 168, 173–203.
Zhang, L.J., Xu, X.M., He, H.J., 2009. POC content in size-fractioned TSS and transportation character in the yellow river. Environ. Sci. 30 (2), 342–347.
Zhang, L.J., Wang, L., Cai, W.J., Liu, D.M., Yu, Z.G., 2013. Impact of human activities on organic carbon transport in the yellow river. Biogeosciences 10 (4), 2513–2524.